Eur. Phys. J. A **28**, 271–275 (2006)
DOI 10.1140/epja/i2006-10060-6

THE EUROPEAN PHYSICAL JOURNAL A

Observation of a $\pi h_{9/2} \otimes \nu i_{13/2}$ oblate band in ^{188}Tl

X.H. Zhou[1,a], L. Ma[1], Y.B. Xing[1], Y.H. Zhang[1], Y.X. Guo[1], X.G. Lei[1], C.Y. Xie[1], M. Oshima[2], Y. Toh[2], M. Koizumi[2], A. Osa[2], Y. Hatsukawa[2], M. Sugawara[3], and M.M. Ndontchueng[4]

[1] Institute of Modern Physics, Chinese Academy of Sciences, Lanzhou 730000, PRC
[2] Japan Atomic Energy Research Institute, Tokai, Ibaraki 319-1195, Japan
[3] Chiba Institute of Technology, Narashino, Chiba 275-0023, Japan
[4] University of Douala, P. O. Box 24157, Douala, Cameroon

Received: 14 March 2006 / Revised: 13 June 2006 /
Published online: 3 July 2006 –
Communicated by R. Krücken

Abstract. Excited states in ^{188}Tl have been studied experimentally using the ^{157}Gd(^{35}Cl, 4n) reaction at a beam energy of 170 MeV. A rotational band built on the $\pi h_{9/2} \otimes \nu i_{13/2}$ configuration with oblate deformation has been established for ^{188}Tl. Based on the structure systematics of the oblate $\pi h_{9/2} \otimes \nu i_{13/2}$ bands in the heavier odd-odd Tl nuclei, we have tentatively proposed spin values for the new band in ^{188}Tl. The $\pi h_{9/2} \otimes \nu i_{13/2}$ oblate band in ^{188}Tl shows low-spin signature inversion, and it can be interpreted qualitatively by the two-quasiparticle plus rotor model including a J-dependent p-n residual interaction.

PACS. 21.10.Re Collective levels – 23.20.-g Electromagnetic transitions – 23.20.Lv gamma transitions and level energies – 27.70.+q $150 \leq A \leq 189$

In our recent publication [1], the low-spin signature inversion has been revealed for the $\pi h_{9/2} \otimes \nu i_{13/2}$ oblate band in ^{190}Tl by adopting the results from the α-γ decay work for ^{194}Bi [2]. It is the first experimental observation of low-spin signature inversion for a band associated with the oblate $\pi h_{9/2} \otimes \nu i_{13/2}$ configuration. In this band, the $\alpha^f_{p\text{-}n} = \alpha^f_p + \alpha^f_n = 1/2 + 1/2 = 1$ favored signature branch lies higher in energy than the $\alpha^{uf}_{p\text{-}n} = \alpha^f_p + \alpha^{uf}_n = 1/2 - 1/2 = 0$ unfavored signature branch at low and medium spins, and the signature splitting tends to revert to the normal ordering at higher-spin states. With great efforts for about two decades, the low-spin signature inversion has been systematically observed in deformed odd-odd nuclei throughout the chart of nuclides [3–10], concerning the high-j $\pi g_{9/2} \otimes \nu g_{9/2}$, $\pi h_{11/2} \otimes \nu h_{11/2}$, $\pi h_{11/2} \otimes \nu i_{13/2}$, $\pi h_{9/2} \otimes \nu i_{13/2}$, and $\pi i_{13/2} \otimes \nu i_{13/2}$ configurations. Theoretically, the inversion phenomenon has been interpreted by different models, including the nuclear triaxiality, proton-neutron residual interaction, and etc. [3,6,7,11–14]. Therefore, the extension of systematic occurrence of signature inversion bands might be crucial for a deeper understanding of the low-spin signature inversion phenomenon. Prior to this work, an early in-beam work [15] reported a long-lived isomer with an oblate configuration of $\pi h_{9/2} \otimes \nu i_{13/2}$ in ^{188}Tl, and two γ lines were suggested to be above the isomer.

The excited states in ^{188}Tl were populated via the ^{157}Gd(^{35}Cl, 4n)^{188}Tl reaction. The ^{35}Cl beam was provided by the tandem accelerator at the Japan Atomic Energy Research Institute (JAERI). The target was an isotopically enriched ^{157}Gd metallic foil of 2.0 mg/cm^2 thickness with a 6.5 mg/cm^2 Pb backing. A γ-ray detector array, GEMINI [16], comprising 13 HPGe's with BGO anti-Compton (AC) shields and 3 LOAX detectors being sensitive to low-energy γ-rays, was used. To obtain information concerning transition multipolarities, the detectors were divided into three groups of which the angle positions (and detector number at that angle) were 90° (2), ±72° (6), ±35° (8) with respect to the beam axis. The detectors were calibrated with ^{60}Co, ^{133}Ba, and ^{152}Eu standard sources; typical energy resolution was about 2.0–2.8 keV at FWHM for the 1332.5 keV line. γ-γ-t and X-γ-t coincidence measurements were performed at a beam energy of 170 MeV. A total of about 270×10^6 coincidence events were accumulated. After accurate gain matching, these coincidence events were sorted into a $4k \times 4k$ symmetric E_γ-E_γ matrix for off-line coincidence relationship analysis. In order to extract information concerning γ-ray anisotropies, the coincidence data were sorted into two asymmetric matrices whose x-axis was the γ-ray energy deposited in the detectors at any angles and the y-axis was the γ-ray energy deposited in the detectors at

[a] e-mail: zxh@impcas.ac.cn

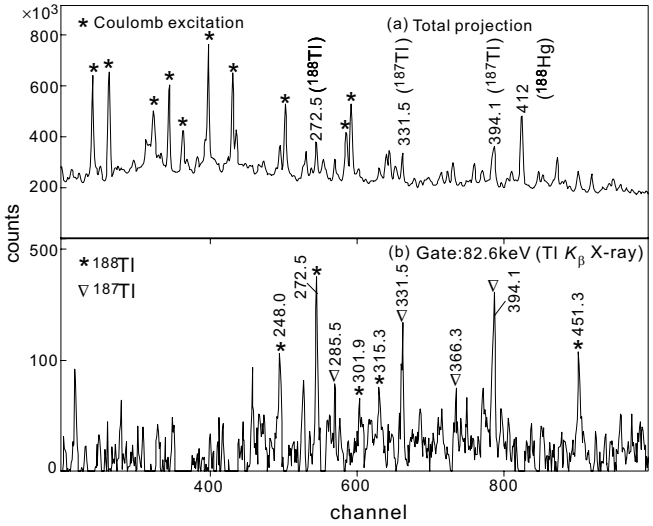

Fig. 1. (a) Part of the total projection spectrum, in which the main products are indicated. (b) The γ-ray spectrum gated by the Tl K_β X-ray.

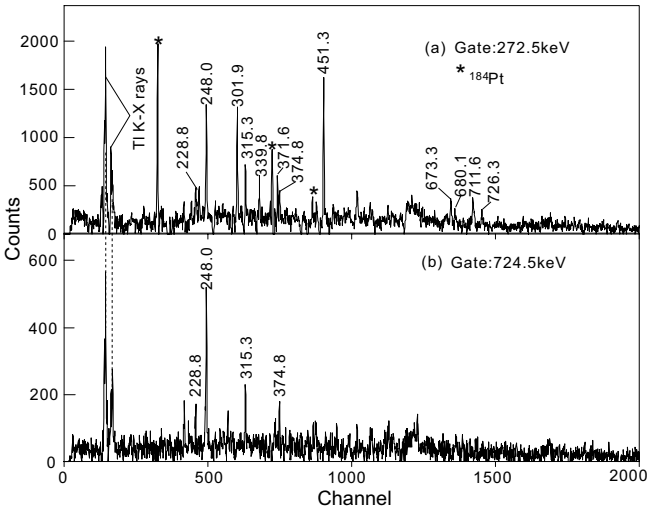

Fig. 2. The γ-ray spectra gated by (a) the 272.5 keV transition, (b) the 724.5 keV transition. Asterisks indicate the contaminant γ-rays (mainly from ^{184}Pt).

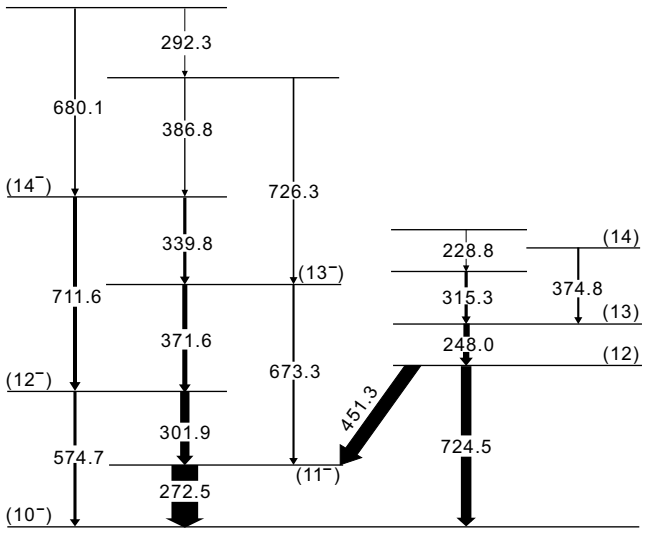

Fig. 3. Level scheme of ^{188}Tl deduced from the present work. The widths of the arrows indicate the relative transition intensities. Tentatively assigned spins are given in parentheses.

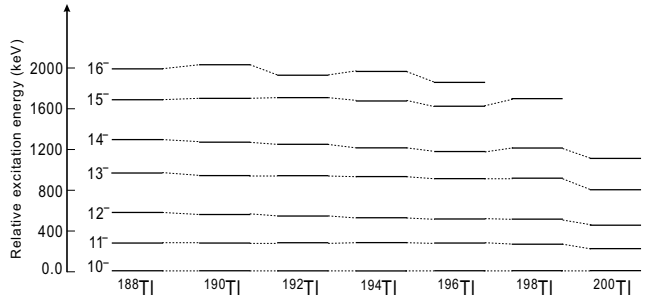

Fig. 4. Systematics of the level structure in the odd-odd $^{188-200}$Tl nuclei.

$\pm 35°$ and 90°, respectively. By gating on the x-axis with suitable γ-rays, two spectra measured at $\pm 35°$ and 90° angle positions were obtained. After correcting for the overall detection efficiency of the detectors at each of the two angles and normalizing the two spectra with respect to each other, γ-ray anisotropy ($R_{ADO}(\gamma)$) was deduced from the intensity ratio in the two spectra. Typical γ-ray anisotropies for the known γ-rays observed in this experiment were 1.3 for stretched quadrupole transitions and 0.7 for stretched pure dipole transitions. Therefore, we assigned the stretched quadrupole transition and stretched dipole transition to the γ-rays of ^{188}Tl with anisotropies around 1.3 and 0.7, respectively.

Assignments of the observed γ-rays to ^{188}Tl were based on the coincidences with the known γ-rays with energies of 272.7 and 301.7 keV [15]. Because of severe competition from fission and many competing evaporation channels open in the present reaction, the γ-ray spectra in this experiment were very complex. As shown in fig. 1(a), the γ-rays from the Coulomb excitation of the target dominate the total projection spectrum; ^{187}Tl, ^{188}Tl and ^{188}Hg were most strongly populated. The assignments were further confirmed by the Tl K_β X-ray coincident information shown in fig. 1(b). A gated spectrum was produced for each of the γ-rays assigned to ^{188}Tl. Typical coincidence spectra are presented in fig. 2. Based on the analysis of the γ-γ coincidence relationships, a level scheme for ^{188}Tl is proposed and shown in fig. 3. The order of transitions in the level scheme is fixed firmly with the help of inter-band transitions. Figure 4 compares the level spacings of the new band observed in ^{188}Tl with those of the $\pi h_{9/2} \otimes \nu i_{13/2}$ oblate bands in the heavier odd-odd Tl isotopes [1,17]. Considering the similarity between the bands observed in odd-odd Tl nuclei, it seems to be reasonable to assign a spin value of 10 for the lowest level shown in fig. 3. If we adopted spin assignments for the bands in odd-odd $^{188-200}$Tl as suggested in fig. 4, the systematic of the level structure in the odd-odd Tl nuclei is very remarkable, *i.e.*, the $\Delta I = 2$ energy spacings and the energy

Table 1. γ-ray transition energies, spin and parity assignments, γ-ray intensities, branching ratios, extracted $B(M1)/B(E2)$ ratios, and γ-ray anisotropies in ^{188}Tl.

E_γ (keV) [a]	$J_i^\pi \rightarrow J_f^\pi$ [b]	I_γ [c]	λ [d]	$B(M1)/B(E2)$ [e]	R_{ADO}
272.5	$(11)^- \rightarrow (10)^-$	100			0.74(7)
301.9	$(12)^- \rightarrow (11)^-$	32			0.72(10)
574.7	$(12)^- \rightarrow (10)^-$	12	0.40(13)	3.0(90)	1.0(20)
371.6	$(13)^- \rightarrow (12)^-$	19			0.73(12)
673.3	$(13)^- \rightarrow (11)^-$	11	0.58(15)	2.58(80)	1.14(16)
339.8	$(14)^- \rightarrow (13)^-$	12			0.71(15)
711.6	$(14)^- \rightarrow (12)^-$	15	1.25(20)	2.16(94)	1.26(18)
386.8		5			
726.3		6			
292.3		$\leq$3			
680.1		7			
248.0	$(13) \rightarrow (12)$	23			0.56(17)
315.3		13			
228.8		4			
374.8	$(14) \rightarrow (13)$	8			0.59(20)
451.3	$(12) \rightarrow (11)^-$	51			1.12(11)
724.5	$(12) \rightarrow (10)^-$	38			1.34(9)

[a] Uncertainties between 0.1 and 0.5 keV.

[b] See text for details about the spin and parity assignments.

[c] Uncertainties between 10 and 30%. Normalized to the 272.5 keV transition.

[d] Branching ratio: $T_\gamma(I \rightarrow I-2)/T_\gamma(I \rightarrow I-1)$, $T_\gamma(I \rightarrow I-2)$ and $T_\gamma(I \rightarrow I-1)$ are the relative γ intensities of the $E2$ and $M1$ transitions depopulating the level I, respectively.

[e] Extracted from the branching ratios assuming $\delta = -0.4$.

staggering between the odd- and even-spin members vary very smoothly from $A = 188$ to 200. Spins for the other levels shown in fig. 3 were proposed from the measured γ-ray anisotropy results.

For the $\Delta I = 1$ negative-parity rotational band shown in fig. 3, the branching ratio, which is defined as

$$\lambda = \frac{T_\gamma(I \rightarrow I-2)}{T_\gamma(I \rightarrow I-1)} \qquad (1)$$

was extracted for strong transitions. Here, $T_\gamma(I \rightarrow I-2)$ and $T_\gamma(I \rightarrow I-1)$ are the γ-ray intensities of the $\Delta I = 2$ and $\Delta I = 1$ transitions, respectively. These intensities were measured in a summed coincidence spectrum gated by the transitions above the state of interest. The branching ratio was used to extract the reduced transition probability ratio, which is defined as [18]

$$\frac{B(M1; I \rightarrow I-1)}{B(E2; I \rightarrow I-2)} = 0.697 \frac{[E_\gamma(I \rightarrow I-2)]^5}{[E_\gamma(I \rightarrow I-1)]^3} \times \frac{1}{\lambda} \frac{1}{1+\delta^2} \left(\frac{\mu_N^2}{e^2 b^2}\right), \qquad (2)$$

where δ is the $E2/M1$ mixing ratio for the $\Delta I = 1$ transitions, and $E_\gamma(I \rightarrow I-1)$ and $E_\gamma(I \rightarrow I-2)$ are the $\Delta I = 1$ and $\Delta I = 2$ transition energies in units of MeV, respectively. The mixing ratios $\delta \approx -0.4$ have been reported for the oblate $\pi h_{9/2} \otimes \nu i_{13/2}$ band in ^{196}Tl [19]. Considering the similar band structure in these Tl isotopes, a constant value $\delta \approx -0.4$ was assumed in the present analysis. The relative intensities for some uncontaminated γ-rays could be measured in the total projection spectrum. Most of the relative intensities were extracted from the spectra gated on the bottom transitions in the band. For some weak γ-rays, only upper limits are given. The relative intensities are corrected with the detection efficiencies. The γ-ray energies, spin and parity assignments, relative γ-ray intensities, branching ratios λ, extracted $B(M1)/B(E2)$ values, and anisotropies ($R_{ADO}(\gamma)$) are collected in table 1.

The $B(M1)/B(E2)$ ratios for a band based on multi-quasiparticle excitation have been proven to be quite useful in characterizing the specific orbitals involved. Information concerning the configuration assignment for the band in ^{188}Tl can be obtained by comparing theoretical $B(M1)/B(E2)$ values with experimental ones. The experimental $B(M1)/B(E2)$ ratios have been deduced according to the eq. (2). Theoretical $B(M1)/B(E2)$ values were calculated according to ref. [1]. The calculated $B(M1)/B(E2)$ ratios are compared with experimental ones in fig. 5 under the assumption of oblate $\pi h_{9/2} \otimes \nu i_{13/2}$ configuration ($\gamma = -60°$) for the band in ^{188}Tl. We used the same parameters as those listed in ref. [1] in the calculations. As shown in fig. 5, the calculations reproduced well the experimental results. Therefore, the band observed in ^{188}Tl likely has the $\pi h_{9/2} \otimes \nu i_{13/2}$ configuration with oblate deformation.

An interesting phenomenon concerning the oblate band in ^{188}Tl is the distinctive energy staggering between the odd- and even-spin members (see fig. 3), indicating an apparent energy signature splitting. If we adopted the configuration and spin-parity assignments proposed in the present work, this staggering reveals that the signature

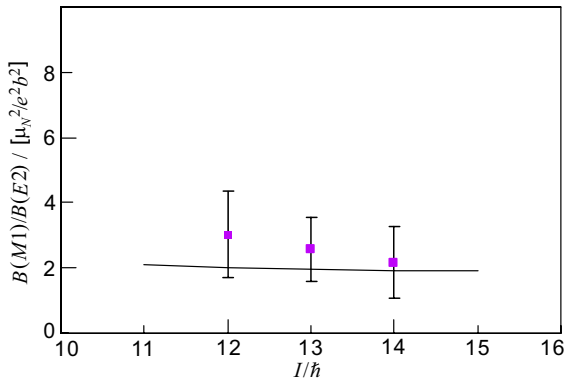

Fig. 5. Experimental $B(M1)/B(E2)$ ratios as a function of the initial spin I for the $\pi h_{9/2} \otimes \nu i_{13/2}$ band, and theoretical prediction assuming $\gamma = -60^\circ$ described in the text.

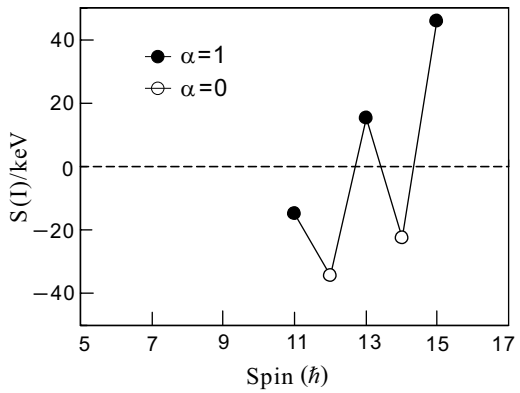

Fig. 6. Signature splitting $S(I)$ as a function of spin I for the $\pi h_{9/2} \otimes \nu i_{13/2}$ oblate band in ^{188}Tl. The filled and open symbols correspond to the favored and unfavored signatures, respectively.

splitting in the $\pi h_{9/2} \otimes \nu i_{13/2}$ band is inverted at low spins; the expected $\alpha^f_{p\text{-}n} = \alpha^f_p + \alpha^f_n = 1/2 + 1/2 = 1$ favored signature branch (odd-spin sequence) lies higher in energy than the $\alpha^{uf}_{p\text{-}n} = \alpha^{uf}_p + \alpha^f_n = 1/2 - 1/2 = 0$ unfavored signature branch (even-spin sequence). Figure 6 presents plot of the signature splitting for the $\pi h_{9/2} \otimes \nu i_{13/2}$ oblate band in ^{188}Tl, defined as $S(I) = E(I) - [E(I+1) - E(I-1)]/2$. As shown in fig. 6, the signature inversion at low-spin regime is distinct. The signature inversion could be interpreted by the residual proton-neutron (p-n) interaction, which attributed the staggering to a J-dependence of the p-n residual interaction ($\vec{J}$ being the total intrinsic angular momentum $\vec{J} = \vec{j_p} + \vec{j_n}$) proposed by Kreiner [17]. If a strong repulsive matrix element of the p-n residual interaction acts in the maximally aligned intrinsic state $J = j_p + j_n = 11$, above the 10^- state a further alignment of the proton and neutron intrinsic spins is energetically more costly and the system prefers to increase its total angular momentum at the expense of collective energy. As a consequence of this, the amplitude of the $J = 11$ component in the wave functions for the 11^- and higher states is drastically reduced and meanwhile the role of the $J = 10$ component becomes dominant [17]. This leads to the energetically favored states with angular momenta $I = R + J = R + 10 =$ even and to the unfavored states being $I - 1 = R + 10 - 1 =$ odd ($R =$ even is the collective angular momentum). Therefore, signature inversion occurs at low spins for this band.

A side cascade, as shown in fig. 3, was observed in ^{188}Tl. However, it is very difficult to associate the experimentally observed states with specific configurations due to the lack of definite spin and parity assignments to these levels.

This work was supported by the National Natural Sciences Foundation of China (Grant No. 10475097, 10375077 and 10221003).

References

1. C.Y. Xie, X.H. Zhou, Y.H. Zhang, Y.X. Guo, X.G. Lei, Y. Zheng, M.L. Liu, L.T. Song, H.L. Wang, W.T. Guo, H.P. Yu, L.H. Zhu, X.G. Wu, F.R. Xu, Phys. Rev. C **72**, 044302 (2005).
2. P. Van Duppen, P. Decrock, P. Dendooven, M. Huyse, G. Reusen, J. Wauters, Nucl. Phys. A **529**, 268 (1991).
3. R. Bengtsson, H. Frisk, F.R. May, J.A. Pinston, Nucl. Phys. A **415**, 189 (1984).
4. Y.H. Zhang, M. Oshima, Y. Toh, X.H. Zhou, M. Koizumi, A. Osa, A. Kimura, Y. Hatsukawa, T. Morikawa, M. Nakamura, M. Sugawara, H. Kusakari, T. Komatsubara, K. Furuno, H.L. Wang, P. Luo, C.S. Wu, F.R. Xu, Phys. Rev. C **68**, 054313 (2003).
5. L.L. Riedinger, H.Q. Jin, W. Reviol, J.-Y. Zhang, R.A. Bark, G.B. Hagemann, P.B. Semmes, Prog. Part. Nucl. Phys. **38**, 251 (1997).
6. M.A. Cardona, A.J. Kreiner, D. Hojman, G. Levinton, M.E. Debray, M. Davidson, J. Davidson, R. Pirchio, H. Somacal, D.R. Napoli, D. Bazzacco, N. Blasi, R. Burch, D. De Acuña, S.M. Lenzi, G. Lo Bianco, J. Rico, C. Rossi Alvarez, Phys. Rev. C **59**, 1298 (1999).
7. R.A. Bark, J.M. Espino, W. Reviol, P.B. Semmes, H. Carlsson, I.G. Bearden, G.B. Hagemann, H.J. Jensen, I. Ragnarsson, L.L. Riedinger, H. Ryde, P.O. Tjøm, Phys. Lett. B **406**, 193 (1997); **416**, 453 (1998).
8. Y. Liu, Y. Ma, H. Yang, S. Zhou, Phys. Rev. C **52**, 2514 (1995).
9. G. García Bermúdez, M.A. Cardona, Phys. Rev. C **64**, 034311 (2001).
10. Y.H. Zhang, F.R. Xu, J.J. He, Z. Liu, X.H. Zhou, Z.G. Gan, T. Hayakawa, M. Oshima, T. Toh, T. Shizuma, J. Katakura, Y. Hatsukawa, M. Matsuda, H. Kusakari, M. Sugawara, K. Furuno, T. Komatsubara, T. Une, S.X. Wen, Z.M. Wang, Eur. Phys. J. A **14**, 271 (2002).
11. K. Hara, Y. Sun, Nucl. Phys. A **531**, 221 (1991).
12. A.K. Jain, A. Goel, Phys. Lett. B **277**, 233 (1992).
13. F.R. Xu, W. Satula, R. Wyss, Nucl. Phys. A **669**, 119 (2000).
14. C. Plettner, I. Ragnarsson, H. Schnare, R. Schwengner, L. Käubler, F. Dönau, A. Algora, G. de Angelis, D.R. Napoli, A. Gadea, J. Eberth, T. Steinhardt, O. Thelen, M. Hausmann, A. Müller, A. Jungclaus, K.P. Lieb, D.G. Jenkins, R. Wadsworth, A.N. Wilson, Phys. Rev. Lett. **85**, 2454 (2000).

15. A.J. Kreiner, C. Baktash, G. García Bermúdez, M.A.J. Mariscotti, Phys. Rev. Lett. **47**, 1709 (1981).
16. K. Furuno, M. Oshima, T. Komatsubara, K. Furutaka, T. Hayakawa, M. Kedera, Y. Hatsukawa, M. Matsuda, S. Mitarai, T. Shizuma, T. Saitoh, N. Hashimoto, H. Kusakari, M. Sugawara, T. Morikawa, Nucl. Instrum. Methods A **421**, 211 (1999).
17. A.J. Kreiner, Phys. Rev. C **22**, 2570 (1980).
18. S. Juutinen, P. Ahonen, J. Hattula, R. Julin, A. Pakkanen, A. Virtanen, J. Simpson, R. Chapman, D. Clarke, F. Khazaie, J. Lisle, J.N. Mo, Nucl. Phys. A **526**, 346 (1991).
19. A.J. Kreiner, M. Fenzl, W. Kutschera, Nucl. Phys. A **308**, 147 (1978).